View metadata, citation and similar papers at core.ac.uk
brought to you by CORE
provided by Repositório Institucional da Universidade de Aveiro

Broadband polarization pulling using Raman amplification

Nelson J. Muga,[1,2,*] **Mário F. S. Ferreira,**[2] **and Armando N. Pinto**[1,3]

[1]*Instituto de Telecomunicações, Campus de Santiago, 3810-193 Aveiro, Portugal*
[2]*Department of Physics, University of Aveiro, Campus de Santiago, 3810-193 Aveiro, Portugal*
[3]*Department of Electronic, Telecommunications, and Informatics, University of Aveiro, Campus de Santiago, 3810-193 Aveiro, Portugal*

**muga@av.it.pt*

Abstract: The Raman gain based polarization pulling process in a copropagating scheme is investigated. We map the degree of polarization, the angle between the signal and pump output Stokes vectors, the mean signal gain and its standard deviation considering the entire Raman gain bandwidth. We show that, in the undepleted regime (signal input power $\sim 1\ \mu$W), the degree of polarization is proportional to the pump power and changes with the signal wavelength, following the Raman gain shape. In the depleted regime (signal input power $\gtrsim$ 1mW), the highest values for the degree of polarization are no more observed for the highest pump powers. Indeed, we show that exists an optimum pump power leading to a maximum degree of polarization.

© 2011 Optical Society of America

OCIS codes: (060.2310) Fiber optics; (260.5430) Polarization; (190.4370) Nonlinear optics, fibers; (230.1150) All-optical devices

References and links

1. M. Martinelli, P. Martelli, and S. M. Pietralunga, "Polarization stabilization in optical communications systems," J. Lightwave Technol. **24**, 4172–4183 (2006).
2. J. E. Heebner, R. S. Bennink, R. W. Boyd, and R. A. Fisher, "Conversion of unpolarized light to polarized light with greater than 50% efficiency by photorefractive two-beam coupling," Opt. Lett. **25**, 257–259 (2000).
3. S. Pitois, A. Picozzi, G. Millot, H. R. Jauslin, and M. Haelterman, "Polarization and modal attractors in conservative counterpropagating four-wave interaction," Europhys. Lett. **70**, 88 (2005).
4. E. Assémat, S. Lagrange, A. Picozzi, H. R. Jauslin, and D. Sugny, "Complete nonlinear polarization control in an optical fiber system," Opt. Lett. **35**, 2025–2027 (2010).
5. J. Fatome, S. Pitois, P. Morin, and G. Millot, "Observation of light-by-light polarization control and stabilization in optical fibre for telecommunication applications," Opt. Express **18**, 15311–15317 (2010).
6. V. V. Kozlov, J. Nuno, J. D. Ania-Castanon, and S. Wabnitz, "Theory of fiber optic Raman polarizers," Opt. Lett. **35**, 3970–3972 (2010).
7. S. Pitois, J. Fatome, and G. Millot, "Polarization attraction using counter-propagating waves in optical fiber at telecommunication wavelengths," Opt. Express **16**, 6646–6651 (2008).
8. Q. Lin and G. P. Agrawal, "Statistics of polarization dependent gain in fiber-based Raman amplifiers," Opt. Lett. **28**, 227–229 (2003).
9. M. Martinelli, M. Cirigliano, M. Ferrario, L. Marazzi, and P. Martelli, "Evidence of Raman-induced polarization pulling," Opt. Express **17**, 947–955 (2009).
10. V. V. Kozlov, J. Nuno, J. D. Ania-Castanon, and S. Wabnitz, "Theoretical study of optical fiber Raman polarizers with counterpropagating beams," J. Lightwave Technol. **29**, 341–347 (2011).
11. L. Ursini, M. Santagiustina, and L. Palmieri, "Raman nonlinear polarization pulling in the pump depleted regime in randomly birefringent fibers," IEEE Photon. Technol. Lett. **23**, 254–256 (2011).
12. A. Galtarossa, L. Palmieri, M. Santagiustina, and L. Ursini, "Polarized backward Raman amplification in randomly birefringent fibers," J. Lightwave Technol. **24**, 4055–4063 (2006).

#149129 - $15.00 USD Received 13 Jun 2011; revised 12 Aug 2011; accepted 15 Aug 2011; published 9 Sep 2011
(C) 2011 OSA

13. M. Fugihara and A. N. Pinto, "Low-cost Raman amplifier for CWDM systems," Microw. Opt. Technol. Lett. **50**, 297–301 (2008).
14. M. Fugihara and A. N. Pinto, "Attenuation fitting functions," Microw. Opt. Technol. Lett. **51**, 2294–2296 (2009).
15. N. J. Muga, M. C. Fugihara, Mário F. S. Ferreira, and A. N. Pinto, "Non-Gaussian ASE noise in Raman amplification systems," J. Lightwave Technol. **27**, 3389–3398 (2009).

1. Introduction

All-optical polarization control schemes can found a large variety of applications in areas like all-optical signal processing and high-speed optical communications systems. Such polarization controllers provide a very fast response time, overcoming an important drawback of polarization control schemes based on optoelectronic elements [1]. Besides that, the possibility to convert unpolarized light to polarized light with unitary efficiency in terms of energy represents a huge advantage over the standard polarizers that waste 50% of the unpolarized light. The lossless repolarization was originally proposed in the context of the noninstantaneous photorefractive effect [2], and of the instantaneous four-wave mixing interaction process [3]. More recently, the all-optical polarization control has been explored in optical fibers through four-wave mixing and stimulated Raman scattering effects [4–6]. Based on the four-wave mixing effect, the state of polarization (SOP) control has been achieved by launching two intense counterpropagating waves in an optical fiber [5, 7]. On the other hand, the SOP control through the stimulated Raman scattering effect has been obtained by copropagating or counterpropagating a pump wave with a weak signal. In this case, the polarization control is assisted by signal amplification [6]. In fact, the pump wave can lead to a preferred amplification of one particular polarization component of the propagating signal [8], giving rise to the pulling of the signal SOP. Raman induced polarization pulling was experimentally verified in [9], using a Raman pump copropagated with a weak signal in a dispersion shifted fiber. Fiber optic Raman polarizers were analyzed theoretically in copropagating [6] and counterpropagating [10] schemes, considering a two beam interaction through Kerr and Raman effects. More recently, an analysis of pump depletion effect on the performance of the polarization pulling process was presented in [11]. All these analyzes consider a single signal-pump frequency difference (13.2 THz) corresponding to the maximum Raman gain.

In our analysis, we consider the effect of detuning the signal from the peak of the Raman gain in a copropagating scheme. Using a broadband model, we show that the preferred amplification of one particular polarization component of the signal allows effective polarization pulling over a wavelength range of 60 nm (7.5 THz). We map parameters like the degree of polarization (DOP), the mean angle between the output signal SOP and the output pump SOP, the mean gain and its standard deviation for the entire Raman gain bandwidth. We show that in the undepleted regime (signal input power $\sim 1\ \mu$W), the DOP at the output, corresponding to an unpolarized input signal, increases with the pump power for the entire Raman gain band. In the depleted regime (signal input power $\gtrsim 1$ mW), this behavior is observed only when the signal wavelength is far away from the Raman gain peak. For signal wavelengths near to the Raman gain peak (in a range of approximately 25 nm), there is an optimum pump power leading to a maximum DOP.

2. Broadband propagation model

The evolution along the fiber of the pump and signal Stokes vectors, $\vec{P}$ and $\vec{S}$, respectively, can be described by the following coupled differential vector equations in the Stokes space [8],

$$d\vec{P}/dz = -\alpha(\omega_p)\vec{P} - \omega_p/(2\omega_s)g_R(\Omega)(|\vec{P}|\vec{S} + |\vec{S}|\vec{P}) + (\omega_p\vec{b} + \gamma_p\vec{W}_p^{NL}) \times \vec{P}, \quad (1)$$

$$d\vec{S}/dz = -\alpha(\omega_s)\vec{S} + 1/2g_R(\Omega)(|\vec{S}|\vec{P} + |\vec{P}|\vec{S}) + (\omega_s\vec{b} + \gamma_s\vec{W}_s^{NL}) \times \vec{S}, \quad (2)$$

#149129 - $15.00 USD Received 13 Jun 2011; revised 12 Aug 2011; accepted 15 Aug 2011; published 9 Sep 2011
(C) 2011 OSA

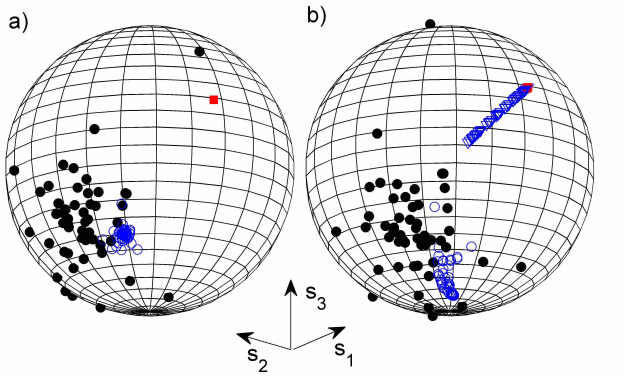

Fig. 1. (a) - Undepleted regime (signal input power equal to 1μW): output pump SOP is represented as a filled square. (b) - Depleted regime (signal input power equal to 1mW): output pump SOPs are represented as filled squares (for $\lambda_s = 1510$ nm) and empty triangles (for $\lambda_s = 1550$ nm). Output SOPs corresponding to unpolarized input signals (SOPs uniformly distributed over the Poincaré sphere) at wavelengths $\lambda_s = 1510$ nm and $\lambda_s = 1550$ nm are represented as filled and empty circles, respectively. Pump at wavelength $\lambda_p = 1450$ nm, input SOP equal to (0,1,0), and optical power equal to 8 W.

where $\alpha(\omega_p)$ and $\alpha(\omega_s)$ are the fiber losses, at pump, ω_p, and signal, ω_s, frequencies, respectively, $g_R(\Omega)$ is the Raman gain coefficient for a pump-signal frequency difference equal to $\Omega = \omega_p - \omega_s$, γ_p and γ_s are the pump and signal nonlinear coefficients, respectively, and $\vec{b}$ is the ratio between the linear birefringence vector and the angular frequency. The linear birefringence vector is given by $\vec{\beta} = \omega\vec{b} = (\beta_1, \beta_2, 0)$, where the two non-null components, β_1 and β_2, are obtained from the birefringence random modulus model [12], i.e., they are modeled as a Langevin process,

$$d\beta_i/dz = -\rho\beta_i + \sigma\eta_i, \quad i = 1,2 \tag{3}$$

where η_i is a Gaussian white noise function with zero mean and variance equal to 1, $\sigma = 2\pi/(L_B\sqrt{L_C})$, and $\rho = 1/L_C$, where L_B and L_C are the beat and correlation lengths, respectively, for the angular frequency ω [12]. The PMD coefficient can be expressed as a function of these two characteristic lengths as $D_p = 16\sqrt{L_C}/(\sqrt{3}\omega L_B)$ [12]. Vectors $\vec{W}_p^{NL} = 2/3(-2S_1, -2S_2, P_3)$ and $\vec{W}_s^{NL} = 2/3(-2P_1, -2P_2, S_3)$ account for the nonlinear polarization rotation of the pump and signal waves, respectively, where P_i, and S_i, with $i = 1,2,3$, are the components of the pump and signal Stokes vectors, respectively. The Raman gain coefficient is modeled as [13],

$$g_R(\Omega) = \sum_{i=1}^{N} a_i \exp\left(-\frac{(\Omega - m_i)^2}{2\sigma_i^2}\right), \tag{4}$$

where a_i, m_i, and σ_i represent, respectively, the amplitude, central position and root-mean-square width of the ith Gaussian function. The frequency dependence of fiber losses is obtained following the model presented in [14],

$$\alpha(\omega) = \alpha_R(\omega) + \alpha_{OH}(\omega) + \alpha_{WG}(\omega) + \alpha_{IR}(\omega) + \alpha_{UV}(\omega), \tag{5}$$

where the first, second, third, fourth and fifth terms on the right hand side correspond, respectively, to the Rayleigh scattering, waveguide imperfections, ion OH^- absorption, infrared absorption, and ultraviolet absorption contributions to fiber losses.

#149129 - $15.00 USD Received 13 Jun 2011; revised 12 Aug 2011; accepted 15 Aug 2011; published 9 Sep 2011
(C) 2011 OSA

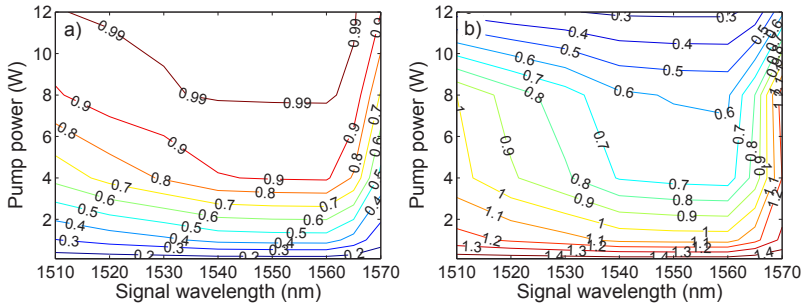

Fig. 2. (a) - Signal output DOP contour map; (b) - Contour map of the mean angle in radians between the signal and pump output Stokes vectors. Signal input DOP equal to 0, signal input power equal to 1 μW, and pump wavelength equal to 1450 nm.

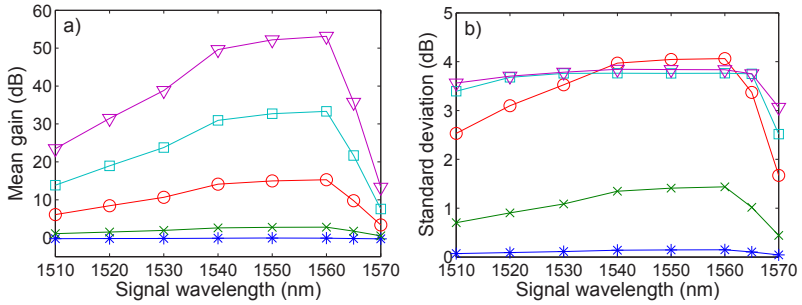

Fig. 3. (a) - Mean signal gain; (b) - Standard deviation gain. Input signal power equal to 1 μW, pump wavelength equal to 1450 nm, and pump powers equal to 0.1, 1, 4, 8 and 12 W (asterisks, crosses, circles, squares and triangles, respectively).

3. Results and discussion

The fiber birefringence evolution was calculated by solving Eq. (3) with a step of 0.4 m. Eqs. (1) and (2) were solved using the fifth-order Runge-Kutta method. The following general parameters were used in this work: $L = 2$ km, $L_C = 10$ m, $L_B = 354$ m (which gives $D_p = 0.0021$ ps/km$^{1/2}$ @1550 nm), $\gamma_p \sim \gamma_s = 2 \times 10^{-3}$ W^{-1}m^{-1}, and Raman gain described by $N = 14$ Gaussian functions, whose parameters can be found in [15]. The pump wavelength and pump input SOP were fixed at $\lambda_p = 1450$ nm and $\hat{p} = (0,1,0)$, respectively. The signal wavelength λ_s was swept from 1510 to 1570 nm. For each signal wavelength, we modeled an unpolarized input signal through the generation of 50 random points over the Poincaré sphere. We have calculated the DOP of the signal, the mean signal gain, the respective standard deviation, and the mean angle between the signal and pump output Stokes vectors. The output DOP was calculated as $DOP = (\langle s_1\rangle^2 + \langle s_2\rangle^2 + \langle s_3\rangle^2)^{1/2}$, where $\langle s_i\rangle$, $i = 1,2,3$, represents the average over the ensemble of signal SOPs, with $s_i = S_i/S_0$, where S_0 is the signal power.

Different signal-pump wavelength separations result in different SOP pulling efficiencies. This outcome can be observed in Fig. 1(a), where two ensembles of output signal SOPs are presented, corresponding to two different signal wavelengths. Results show a stronger SOP pulling for the wavelength where the Raman gain is higher, i.e., $\lambda_s = 1550$ nm. We calculate the DOP for the different pump powers and signal wavelengths (see Fig. 2(a)). The DOP increases with the pump power, reaching values close to 1 over the entire wavelength range considered (from 1510 to 1570 nm). These high DOP values are more difficult to reach for signal wavelengths

#149129 - $15.00 USD Received 13 Jun 2011; revised 12 Aug 2011; accepted 15 Aug 2011; published 9 Sep 2011
(C) 2011 OSA

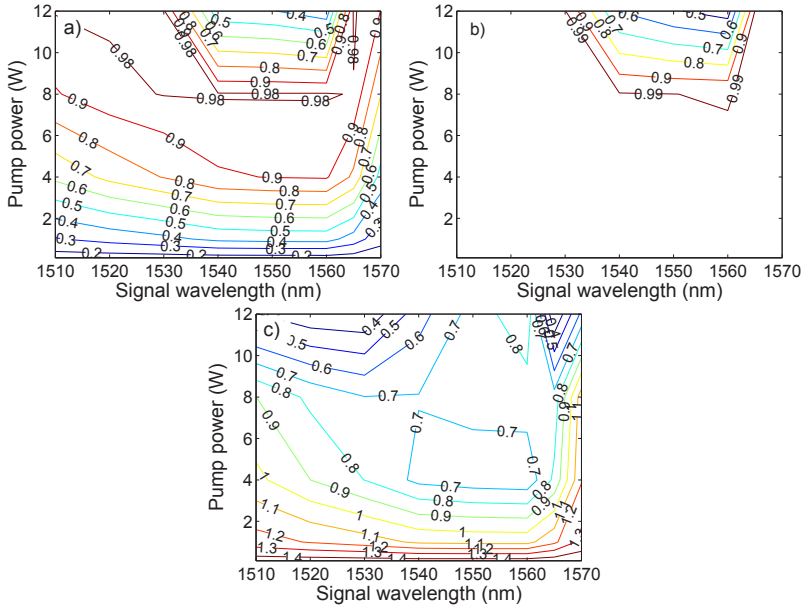

Fig. 4. (a) - Signal output DOP contour map; (b) - Pump output DOP contour map; (c) - Contour map of the mean angle in radians between the signal and pump output Stokes vectors. Signal input DOP equal to 0, signal input power equal to 1 mW, pump input DOP equal to 1, and pump wavelength equal to 1450 nm.

far away from the maximum Raman gain. In such cases, higher pump powers are required. The contour map presented in Fig. 2(b) shows that the smallest mean angles between the signal and pump Stokes vectors occur for the highest pump powers: for pump powers $\geq$ 9 W and signal wavelengths around 1550 nm the mean angle takes values smaller than 0.5 rad. Figures 3(a) and 3(b) show, respectively, the mean signal gain and the respective standard deviation. We should note that in a low PMD scenario, Raman gain is quite high because signal tends to be copolarized with respect to the pump. We observe from Fig. 3(a) that the mean gain increases with the pump power, presenting a well-known spectrum shape. The highest gain deviations are observed for wavelengths near the maximum mean gain, see Fig. 3(b).

In order to explore the Raman induced SOP pulling process in a depleted regime, we increased the signal power to 1 mW. For this new scenario, the pulling SOP process is quantitative and qualitatively different of that observed in the previous case. We found that for pump powers $\geq$ 8 W and high Raman gains the output pump SOP becomes dependent on the input signal SOP. Figure 1(b) shows the pump and signal output SOPs, considering a pump power equal to 8 W. For $\lambda_s = 1510$ nm the output pump SOP remains fixed, whereas for $\lambda_s = 1550$ nm it takes different values for different input signal SOPs. On the other hand, Fig. 4(a) shows that the highest DOP values are no more observed for the highest pump powers. For signal wavelengths between 1535 and 1560 nm, the highest DOP values are observed around 8 W. Figure 4(b) shows that the pump DOP becomes smaller than one for pump powers higher than 8 W and signal wavelengths between 1535 and 1560 nm. This result is in agreement with [11]. The small mean angle values occur for high pump powers but for signal wavelengths around 1525 nm, see Fig. 4(c). Due to pump depletion, the signal gain at the highest pump powers is smaller than that observed in the previous case (see Fig. 5(a) and Fig. 3(a), respectively). On the other hand, Fig. 5(b) shows that the smallest standard deviations occur around 1550 nm for

#149129 - $15.00 USD Received 13 Jun 2011; revised 12 Aug 2011; accepted 15 Aug 2011; published 9 Sep 2011
(C) 2011 OSA

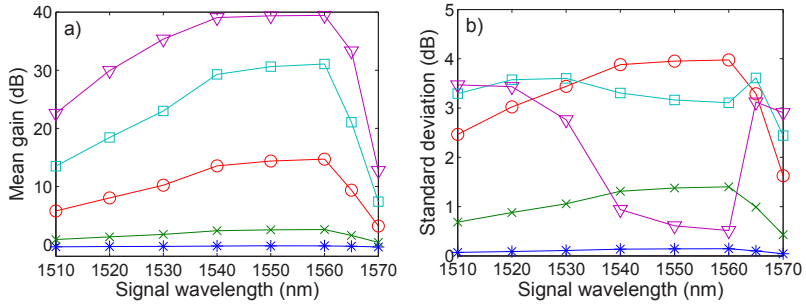

Fig. 5. (a) - Mean signal gain. (b) - Standard deviation gain. Signal input power equal to 1 mW, pump wavelength equal to 1450 nm, and pump powers equal to 0.1, 1, 4, 8 and 12 W (asterisks, crosses, circles, squares and triangles, respectively).

pump powers higher than 4 W. This means that pump depletion makes the signal gain independent of the input signal SOP. Although not presented here, we have carried out simulations for $L_B = 35$ m ($D_p = 0.022$ ps/km$^{1/2}$) in both depleted and undepleted pump regimes. Our results showed that the Raman pulling process efficiency remains stable into the considered range of PMD values, i.e., from 0.0021 up to 0.022 ps/km$^{1/2}$, for both pump regimes.

We modeled pump and signal as continuous waves, neglecting the walk-off effect between pump and signal. Nevertheless, the signal DOP will certainly be influenced by pump power fluctuations. Our signal DOP maps, presented in Fig. 2(a) and Fig. 4(a), show that the domains of smallest gradients (along the y direction - pump power) tend to correspond to the highest DOP values. Therefore, systems operating with a Raman pump in such power range will tend to present an enhanced signal DOP tolerance with respect to pump power fluctuations. Therefore, the signal DOP dependence of pump power fluctuations can in principle be mitigated by choosing an appropriate pump power.

4. Conclusions

We showed that all-optical polarization control based on Raman scattering can be obtained over a wavelength range of 60 nm. The efficiency of the pulling process is higher close to the Raman gain peak, where the DOP is roughly constant for a wavelength range of 15 nm. For shorter and longer wavelengths, higher pump powers are required in order to assure maximum efficiencies: for instance, a DOP equal to 0.9 is obtained at 1550 nm for a pump power around 4 W, whereas the double power is needed in order to obtain the same DOP at 1510 nm, considering $\lambda_p =$ 1450 nm. In spite of the random pump SOP evolution along the propagation, we found that the mean angle between the output signal and pump Stokes vectors becomes smaller when the signal output DOP is close to 1. The output pump SOP information can therefore be used in order to operate on the output signal SOP. Different results were found in the depleted regime, where the highest DOP values are no more observed for the highest pump powers. For signal wavelengths between 1535 and 1560 nm, the highest DOP values occur for a optimum pump power, which in our case was 8 W. For powers higher than the optimum value, the polarization pulling effect becomes less efficient due to the decrease of the pump DOP.

Acknowledgement

This work was supported in part by supported by Fundação para a Ciência e Tecnologia, under the PhD Grant SFRH/BD/28275/2006, and the ”QuantPrivTel-PTDC/EEA-TEL/103402/2008” and ”OSP-HNLF-PTDC/EEA-TEL/105254/2008” projects.

#149129 - $15.00 USD Received 13 Jun 2011; revised 12 Aug 2011; accepted 15 Aug 2011; published 9 Sep 2011
(C) 2011 OSA